

# The effect of starvation on the dynamics of consumer populations

Justin D. Yeakel \* †‡, Christopher P. Kempes †, and Sidney Redner †§

\* School of Natural Science, University of California Merced, Merced, CA, †The Santa Fe Institute, Santa Fe, NM, §Department of Physics, Boston University, Boston

MA, and ‡ To whom correspondence should be addressed: jdyeakel@gmail.com

Submitted to Proceedings of the National Academy of Sciences of the United States of America

## This is the abstract.

The behavioral ecology of most, if not all, organisms is influenced by the energetic state of individuals, which directly influences how an organism invests its reserves in an uncertain environment. Such behaviors are generally manifested as trade-offs between investing in individual maintenance and growth (somatic effort) or allocating energy towards reproduction (reproductive effort) [1, 2, 3]. The timing of these behaviors is often important and is under strong selective pressure, as they tend to have large effects on the future fitness of the organism [4]. To what extent, and when, organisms invest in somatic vs. reproductive expenditures may be driven by habitat, seasonality, evolutionary history, inter- or intra-specific interactions, and the distribution of resources. Importantly, the influence of resource limitation on an organism's ability to maintain its nutritional stores may lead to repeated delays or shifts in reproduction over the course of an organism's life.

Maximizing fitness between growth and maintenance activities vs. reproductive efforts in large part structures the life-history of species, and this can be achieved by alternative behavioral strategies or via changes in physiology, both of which are sensitive to resource availability. Behavioral changes in somatic or reproductive investment often occur in response to limited resources [5]. For example, reindeer invest less in calves born after harsh winters (when the mother's energetic state is poor) than in calves born after moderate winters [6], whereas many bird species invest differently in broods during periods of resource scarcity [7, 8], sometimes delaying or foregoing reproduction for a breeding season (capital breeding) [1, 9, 10]. Even freshwater and marine zooplankton have been observed to avoid reproduction under nutritional stress [11], with those that do reproduce evincing lower survival rates [2], while artificially induced stress has been observed to decrease reproductive success in Atlantic cod [12]. Organisms may also separate maintenance and growth from reproduction over space and time: many salmonids, birds, and some mammals return to migratory breeding grounds to reproduce after one or multiple seasons in alternative environments spent accumulating body mass and nutritional reserves [13, 14, 15].

Physiological mechanisms also play an important role in regulating reproductive expenditures during periods of resource limitation. Diverse mammals (47 species in 10 families) exhibit delayed implantation whereby females postpone fetal development (blastocyst implantation) to time with accumulation of nutritional reserves [16, 17]. Furthermore, many mammals (including humans) suffer irregular menstrual cycling and higher abortion rates during periods of nutritional stress [18, 19]. In the extreme case of unicellular organisms, nutrition is unavoidably linked to reproduction because the nutritional state of the cell regulates all aspects of the cell cycle [20]. The existence of so many independently evolved mechanisms across such a diverse suite of organisms points to the importance and universality of the fundamental tradeoff between somatic and reproductive investment, however the dynamic implications of these constraints are unknown.

Though straightforward conceptually, incorporating the energetic dynamics of individuals [21] into a population-level framework [21, 22] presents numerous mathematical obstacles (in particular a lack of smoothness or differentiability [23]), and often suffers from over-fitting due to an overabundance of parameters. An alternative approach involves modeling the macroscale relationships that guide somatic vs. reproductive investment in a consumer-resource system. Macroscale Lotka-Volterra models assume a dependence of consumer population growth rates on resource density, thus implicitly incorporating the requirement of resource availability for reproduction [24]. Resource limitation and the subsequent effects of starvation may be alternatively accounted for explicitly, such that reproduction is permitted only for individuals with sufficient energetic reserves. This permits us to incorporate *i*) the reproductive time lag that is sensitive to changing rates of starvation and recovery, and *ii*) the idea that reproduction is strongly allo-metrically constrained [3], and is not generally a linear function of resource density.

## Starvation dynamics

We explore how the energetic tradeoff between maintaining and building somatic tissue vs. reproduction can influence the dynamics of populations, and how such dynamics may be constrained by allometry. We begin by establishing a minimal Nutritional State-structured population Model (NSM), where the consumer population is divided into two energetic states: *i*) an energetically replete (full) state  $F$ , where the consumer reproduces at a constant rate  $\lambda$ , and *ii*) an energetically deficient (hungry) state  $H$ , where reproduction is suppressed, and mortality occurs at rate  $\mu$ . The resource  $R$  has logistic growth with a linear growth rate  $\alpha$  and carrying capacity of unity. Consumers transition from state  $F$  to state  $H$  by starvation at rate  $\sigma$  and in proportion to the lack of resources  $(1 - R)$ . Conversely, consumers recover from state  $H$  to the full state  $F$  at rate  $\rho$  and in proportion to  $R$ . Resources are eliminated by the consumer in both states: by energetically deficient consumers at rate  $\rho$ , and by energetically replete consumers at rate  $\beta$ . Accordingly, the system of equations is written

$$\begin{aligned}\dot{F} &= \lambda F + \rho RH - \sigma(1 - R)F, \\ \dot{H} &= \sigma(1 - R)F - \rho RH - \mu H, \\ \dot{R} &= \alpha R(1 - R) - R(\rho H + \beta F).\end{aligned}\quad [0]$$

## Reserved for Publication Footnotes

100 There are three steady states for the NSM: two trivial fixed points at  $(R^* = 0, H^* = 0, F^* = 0)$  and  $(R^* = 1, H^* = 0, F^* = 0)$ , and one non-trivial internal fixed point at

$$F^* = \frac{\alpha\lambda\mu(\mu + \rho)}{(\lambda\rho + \mu\sigma)(\lambda\rho + \mu\beta)},$$

$$H^* = \frac{\alpha\lambda^2(\mu + \rho)}{(\lambda\rho + \mu\sigma)(\lambda\rho + \mu\beta)},$$

$$R^* = \frac{\mu(\sigma - \lambda)}{\lambda\rho + \mu\sigma}.$$
[0]

103 Because there is only one internal fixed point, as long as it is  
 104 stable the population trajectories will serve as a global attractor  
 105 for any set of positive initial conditions. In a multidimensional  
 106 system, linear stability is determined with respect to the Ja-  
 107 cobian Matrix  $\mathbf{J}|_*$  (where  $|_*$  denotes evaluation at the internal  
 108 steady state), where each element of the matrix is defined by  
 109 the partial derivative of each differential equation with respect  
 110 to each variable. If the parameters of  $\mathbf{J}|_*$  are such that the real  
 111 part of its leading eigenvalue is  $< 0$ , then the system is stable  
 112 to small pulse perturbations.

### 113 Allometric relationships

114 Our model explores a wide variety of possible dynamics yet we  
 115 have not described the realistic regimes occupied by organisms  
 116 where the challenge is to constrain the covariation of rates. Al-  
 117 lometric scaling relationships highlight common constraints and  
 118 average trends across large ranges in body size and species di-  
 119 versity. Many of these relationships can be derived from a small  
 120 set of assumptions and below we describe a framework for the  
 121 covariation of timescales and rates across the range of mam-  
 122 mals for each of the key parameters of our model. We are able  
 123 to define the regime of dynamics occupied by the entire class  
 124 of mammals along with the key differences between the largest  
 125 and smallest mammals.

126 Nearly all of the rates described in the NSM are to some  
 127 extent governed by consumer metabolism, and thus can be es-  
 128 timated based on known allometric constraints. The scaling  
 129 relationship between an organism's metabolic rate  $B$  and its  
 130 body size at reproductive maturity  $M$  is well documented [25]  
 131 and plays a central role in a variety of scaling relationships.  
 132 Organismal metabolic rate  $B$  is known to scale as  $B = B_0 M^\eta$ ,  
 133 where  $\eta$  is the scaling exponent, generally assumed to be  $3/4$   
 134 for metazoans, and varies in unicellular species between  $\eta \approx 1$   
 135 in eukaryotes and  $\eta \approx 1.76$  in bacteria [?]. Several efforts  
 136 have shown how a partitioning of this metabolic rate between  
 137 growth and maintenance purposes can be used to derive a gen-  
 138 eral equation for the growth trajectories and growth rates of  
 139 organisms ranging from bacteria to metazoans [3]. More specif-  
 140 ically, the interspecific trends in growth rate can be approxi-  
 141 mated by  $\lambda = \lambda_0 M^{\eta-1}$ . This relationship is derived from the  
 142 simple balance

$$B_0 m^\eta = E_m \frac{dm}{dt} + B_m m$$
[0]

143 [a and b notation — these parameters are easily measured  
 144 bioenergetic parameters which are often approximately invari-  
 145 ant across organisms of vastly different size. Our notation seeks  
 146 to illustrate that the allometric model fundamentally depends  
 147 on a small number of free parameters.] where  $E_m$  is the energy  
 148 needed to synthesize a unit of mass,  $B_m$  is the metabolic rate  
 149 to support an existing unit of mass, and  $m$  is the mass at any  
 150 point in development. It is useful to explicitly write this bal-

151 ance because it can also be modified to understand the rates with  $a = B_0/E_m$ ,  $b = B_m/E_m$ , and  $c = (a/b)^{1/(\eta-1)}$ . We are  
 152 of both starvation and recovery from starvation. [Spell out the  
 153 connection to nutritional state more explicitly] [As we will see  
 154 it is possible to derive both sigma and rho from this balance]

155 For the rate of starvation, we make the simple assumption  
 156 that an organism must meet its maintenance requirements us-  
 157 ing digested mass as the sole energy source. This assumption  
 158 implies the simple metabolic balance

$$\frac{dm}{dt} E'_m = -B_m m$$
[0]

159 where  $E'_m$  is the amount of energy stored in a unit of existing  
 160 body mass which may differ from  $E_m$ , the energy required to  
 161 synthesis a unit of biomass. Give the adult mass,  $M$ , of an  
 162 organism this energy balance prescribes the mass trajectory of  
 163 a starving organism:

$$m(t) = M e^{-B_m t / E'_m}.$$
[0]

164 Considering that only certain tissues can be digested for energy,  
 165 for example the brain cannot be degraded to fuel metabolism,  
 166 we define the rate for starvation and death by the timescales  
 167 required to reach specific fractions of normal adult mass. We  
 168 define  $m_{starve} = \epsilon M$  where it could be the case that organisms  
 169 have a systematic size-dependent requirement for essential tis-  
 170 sues, such as the minimal bone or brain mass. For example,  
 171 considering the observation that body fat in mammals scales  
 172 with overall body size according to  $M_f = f_0 M^\gamma$ , and assum-  
 173 ing that once this mass is fully digested the organism begins to  
 174 starve, would imply that  $\epsilon = 1 - f_0 M^\gamma / M$ . Taken together the  
 175 time scale for starvation is given by

$$t_\sigma = -\frac{E_m \log(\epsilon)}{B_m}.$$
[0]

176 The starvation rate is  $\sigma = 1/t_\sigma$ , which implies that  $\sigma$  is in-  
 177 dependent of adult mass if  $\epsilon$  is a constant, and if  $\epsilon$  does scale  
 178 with mass, then  $\sigma$  will have a factor of  $1/\log(1 - f_0 M^\gamma / M)$ .  
 179 In either case  $\sigma$  does not have a simple scaling with  $\lambda$  which is  
 180 important for the dynamics that we later discuss.

181 The time to death should follow a similar relationship, but  
 182 defined by a lower fraction of adult mass,  $m_{death} = \epsilon' M$ .  
 183 Consider, for example, that an organism dies once it has di-  
 184 gested all fat and muscle tissues, and that muscle tissue scales  
 185 with body mass according to  $M_{mm} = mm_0 M^\zeta$ , then  $\epsilon' =$   
 186  $1 - (f_0 M^\gamma + mm_0 M^\zeta) / M$ . Muscle mass has been shown to  
 187 be roughly proportional to body mass [?] in mammals and thus  
 188  $\epsilon'$  is effectively  $\epsilon$  minus a constant. Thus

$$t_\mu = -\frac{E_m \log(\epsilon')}{B_m}$$
[0]

189 and  $\mu = 1/t_\mu$ .

190 It should be noted that we have thus far used mammalian  
 191 allometry to describe the size-based relationships for growth,  
 192 starvation, and death. However, our presentation is general,  
 193 and other functional forms for  $\epsilon$ , for example, could be deter-  
 194 mined for other classes of organisms. Considering bacteria, we  
 195 might expect that starvation or death is defined by the complete  
 196 digestion of proteins, and in Table ?? we provide all parameter  
 197 values for bacteria which we later use as a comparison in our  
 198 analysis.

199 The rate of recovery  $\rho = 1/t_\rho$  requires that an organism ac-  
 200 crues tissue from the starving state to the full state. We again  
 201 use the balance given in Equation to find the timescale to re-  
 202 turn to the mature mass from a given reduced starvation mass.  
 203 The general solution to Equation is given by

$$m(t) = c \left[ 1 - \left( 1 - \frac{b}{a} m_0^{1-\eta} \right) e^{-b(1-\eta)t} \right]^{1/(1-\eta)}$$
[0]

204 with  $a = B_0/E_m$ ,  $b = B_m/E_m$ , and  $c = (a/b)^{1/(\eta-1)}$ . We are  
 205 then interested in the timescale,  $t_\rho = t_2 - t_1$ , which is the time

it takes to go from  $m(t_1) = \epsilon M$  to  $m(t_2) = M$ , which has the final form of

$$t_\rho = \frac{\log(1 - (cM)^{1-\eta}) - \log(1 - (ceM)^{1-\eta})}{(\eta - 1)b}. \quad [0]$$

Although these rate equations are general and will hold for any organism, here we focus on parameterizations for terrestrial-bound endotherms, specifically mammals, which range from  $M \approx 1$  gram (the Etruscan shrew *Suncus etruscus*) to  $M \approx 10^7$  grams (the late Eocene to early Miocene Indricotheriinae). Investigating other classes of organisms requires only substituting the energetic and scale parameters shown in Table 1.

### The stabilizing effects of allometric constraints

Stability in the NSM is conditioned on the consumer's starvation rate  $\sigma$  relative to its reproduction rate  $\lambda$ . If  $\sigma < \lambda$ , the resource steady state density is negative and extinction is inevitable. The condition  $\sigma = \lambda$  is a transcritical (TC) bifurcation, thus marking a hard boundary below which the system is unphysical due to the unregulated growth of the consumer population. That the timescale of reproduction is larger than the timescale of starvation is intuitive for macroscopic organisms, as the rate at which one loses tissue due to a lack of resources is generally much faster than reproduction. In fact, allometric derivations for both reproduction [3] and starvation (Eq. ??) show that this relationship always holds for organisms within observed body size ranges (Fig. 2). We note that the asymptote for the starvation rate at  $M \approx 6.16 \times 10^7$  defines the mass at which fat and muscle tissue accounts for 100% of organismal weight, thereby placing a hard scaling boundary on our derivation for the starvation rate.

In addition to the hard bound defined by the TC bifurcation, oscillating or cyclic dynamics present an implicit constraint to persistence by increasing the risk of extinction. If cycles are large, stochastic effects may result in extinction in either the consumer or resource population. In continuous-time systems, a stable limit cycle arises when a pair of complex conjugate eigenvalues crosses the imaginary axis to attain positive real parts [26]. This condition, known as a Hopf bifurcation, is defined by  $\text{Det}(\mathbf{S}) = 0$ , where  $\mathbf{S}$  is the Sylvester matrix, which is composed of the coefficients of the characteristic polynomial describing the Jacobian [27]. Moreover, as a non-cyclic stable system nears the Hopf bifurcation, transient or decaying cycles can grow in magnitude, despite the existence of a positive, non-cyclic, steady state density. Given that ecological systems exist in a state of constant perturbation [28], even the onset of transient cycles that decay over time can increase the risk of extinction [29, 30, 31], such that the distance of a system from the Hopf bifurcation, even in the stable region, is relevant to persistence.

The NSM exhibits both non-cyclic as well as cyclic dynamics, and which behavior dominates depends strongly on the rate of starvation  $\sigma$  relative to the rate of recovery  $\rho$ . Although starvation leads to mortality risk for the individual, a moderate amount promotes persistence of both consumer and resource populations. Non-cyclic stability of the fixed point generally requires a higher starvation rate  $\sigma$  relative to the recovery rate  $\rho$ . The intuition behind this is that transition to the hungry (non-reproductive) state permits the resource to recover and transient dynamics to subside, whereas a low  $\sigma$  overloads the system with energetically-replete (reproducing) individuals, thus producing maintained oscillations between consumer and resource (Fig. ??). However if  $\sigma$  is too large, mortality due to starvation depletes the consumer population, resulting in a lower steady state density for the consumer and an opposingly higher steady state density for the resource.

Whereas the rate of consumer growth defines a hard bound of biological feasibility (the TC bifurcation), the rate of starva-

tion determines the sensitivity of the consumer population to changes in resource density. While higher rates of starvation result in lower steady state population size – increasing the risk of stochastic extinction – lower rates of starvation result in a system poised near either the TC or Hopf bifurcation (or both), which will lead to elimination of the resource or the development of cyclic oscillations, respectively. Which bifurcation is approached is wholly dependent on the rate of recovery: if it is high, then cyclic dynamics will develop; if it is low, resource extinction becomes increasingly likely.

As the allometric derivations of NSM rate laws reveal,  $\sigma$  and  $\rho$  are not independent parameters, such that the bifurcation space shown in Fig. ?? cannot be freely navigated if assuming biologically reasonable parameterizations. Given the parameterization for terrestrial endotherms shown in Table ?? with mass  $M$  as the only free parameter, rates of starvation and recovery are constrained to a fairly small window of potential values. We find that the allometric constraints given for terrestrial endothermic organisms confine dynamics to the steady state regime across all reasonable body size classes, which for mammals ranges from ca. 1 gram (the Etruscan shrew) to ca.  $10^7$  grams (represented by the Indricotheriinae, a subfamily of mammals living from the mid-Eocene to early Miocene). Moreover, for larger organismal mass, the distance increases between the allometric values for  $\sigma(M)$  and  $\rho(M)$  relative to the Hopf bifurcation, while uncertainty in allometric parameters (20% variation around the mean; Fig. ??) results in little difference in the position of the TC and Hopf bifurcations as well as consumer energetic rates. This result suggests 1) that small mammals are more prone to population oscillations – including both stable limit cycles as well as transient cycles – than large mammals, and 2) the decreasing distance to the Hopf bifurcation with lower body sizes is suggestive of a dynamic barrier to the mass of endothermic organisms. Although the prediction of larger oscillations for animals with smaller body sizes generally holds, empirical observations of large animal population cycles are plagued by long generation times and the influence of top-down effects [REFS] making direct empirical observation problematic.

Higher rates of starvation results in a larger flux of the population to the hungry state, eliminating reproduction and increasing the likelihood of death, however it is the rate of starvation relative to the rate of recovery that determines the long-term dynamics of the system (Fig. ??). By examining the ratio  $\sigma/\rho$ , we can understand the competing effects of cyclic dynamics vs. population density on the probability of extinction. We computed the probability of extinction, which we defined as  $H(t) + F(t) = 10$  at any instant across all values of  $10^3 < t \leq 10^6$ , for 1000 replicates of the continuous-time system shown in Eq. XX for an organism of  $M = 100$ g, assuming random initial conditions around the steady state solution. By allowing the rate of starvation to vary, we assessed extinction risk across a range of values for the ratio  $\sigma/\rho$  varying between  $10^{-2}$  to 2.5, thus examining a vertical cross-section of Fig. ?? As we expected, we found higher rates of extinction for both low and high values of  $\sigma/\rho$ ; for low values the higher extinction risk is the consequence of transient cycles with larger amplitudes as the system nears the Hopf bifurcation. For high values of  $\sigma/\rho$ , higher extinction risk is due to the steady decrease in the steady state consumer population density. This interplay creates an ‘extinction refuge’, such that for a relatively small range of  $\sigma/\rho$ , extinction probabilities are minimized.

As has been described, the  $\sigma$  vs.  $\rho$  space cannot be freely traversed, such that not all values of  $\sigma/\rho$  are biologically feasible. We observe that the allometrically constrained values of  $\sigma/\rho$  (with  $\pm 20\%$  variability around the mean for the energetic parameters used to determine each rate) fall within the extinc-

tion refugia, such that they are close enough to the Hopf bifurcation to avoid low steady state densities, though far enough away to avoid large-amplitude transient cycles. The fact that allometric values of  $\sigma$  and  $\rho$  fall within this relatively small window supports the possibility that a selective mechanism has constrained the physiological conditions driving observed starvation and recovery rates within populations. Such a mechanism would involve a feedback between the dynamics of the population and the fitness of individuals within the population, though to what extent the dynamics of the population influence rates

of starvation and recovery would also involve potential tradeoffs in reproduction and somatic maintenance. Despite the possible mechanisms, our finding that allometrically-determined energetic rates place the system within this low probability of extinction region suggests that the NSM system provides general insight to a phenomena that may both drive – and constrain – natural animal populations.

### Minimizing extinction risk

1. Martin TE (1987) Food as a Limit on Breeding Birds: A Life-History Perspective. *Annu. Rev. Ecol. Syst.* 18:453–487.
2. Kirk KL (1997) Life-History Responses to Variable Environments: Starvation and Reproduction in Planktonic Rotifers. *Ecology* 78:434–441.
3. Kempes CP, Dutkiewicz S, Follows MJ (2012) Growth, metabolic partitioning, and the size of microorganisms. *PNAS* 109:495–500.
4. Mangel M, Clark CW (1988) *Dynamic Modeling in Behavioral Ecology* (Princeton University Press, Princeton).
5. Morris DW (1987) Optimal Allocation of Parental Investment. *Oikos* 49:332.
6. Tveraa T, Fauchald P, Henaug C, Yoccoz NG (2003) An examination of a compensatory relationship between food limitation and predation in semi-domestic reindeer. *Oecologia* 137:370–376.
7. Daan S, Dijkstra C, Drent R, Meijer T (1988) Food supply and the annual timing of avian reproduction.
8. Jacot A, Valcu M, van Oers K, Kempenaers B (2009) Experimental nest site limitation affects reproductive strategies and parental investment in a hole-nesting passerine. *Animal Behaviour* 77:1075–1083.
9. Stearns SC (1989) Trade-Offs in Life-History Evolution. *Funct. Ecol.* 3:259.
10. Barboza P, Jorda D (2002) Intermittent fasting during winter and spring affects body composition and reproduction of a migratory duck. *J Comp Physiol B* 172:419–434.
11. Threlkeld ST (1976) Starvation and the size structure of zooplankton communities. *Freshwater Biol.* 6:489–496.
12. Morgan MJ, Wilson CE, Crim LW (1999) The effect of stress on reproduction in Atlantic cod. *Journal of Fish Biology* 54:477–488.
13. Weber TP, Ens BJ, Houston AI (1998) Optimal avian migration: A dynamic model of fuel stores and site use. *Evolutionary Ecology* 12:377–401.
14. Mduma SAR, Sinclair ARE, Hilborn R (1999) Food regulates the Serengeti wildebeest: a 40-year record. *J. Anim. Ecol.* 68:1101–1122.
15. Moore JW, Yeakey JD, Peard D, Lough J, Beere M (2014) Life-history diversity and its importance to population stability and persistence of a migratory fish: steelhead in two large North American watersheds. *J. Anim. Ecol.*
16. Mead RA (1989) in *Carnivore Behavior, Ecology, and Evolution* (Springer US, Boston, MA), pp 437–464.
17. Sandell M (1990) The Evolution of Seasonal Delayed Implantation. *The Quarterly Review of Biology* 65:23–42.
18. Bulik CM, et al. (1999) Fertility and Reproduction in Women With Anorexia Nervosa. *J. Clin. Psychiatry* 60:130–135.
19. Trites AW, Donnelly CP (2003) The decline of Steller sea lions *Eumetopias jubatus* in Alaska: a review of the nutritional stress hypothesis. *Mammal Review* 33:3–28.
20. Glazier DS (2009) Metabolic level and size scaling of rates of respiration and growth in unicellular organisms. *Funct. Ecol.* 23:963–968.
21. Kooijman SALM (2000) *Dynamic Energy and Mass Budgets in Biological Systems* (Cambridge).
22. Sousa T, Domingos T, Poggiale JC, Kooijman SALM (2010) Dynamic energy budget theory restores coherence in biology. *Philos. T. Roy. Soc. B* 365:3413–3428.
23. Diekmann O, Metz JAJ (2010) How to lift a model for individual behaviour to the population level? *Philos. T. Roy. Soc. B* 365:3523–3530.
24. Murdoch WV, Briggs CJ, Nisbet RM (2003) *Consumer-resource Dynamics*, Monographs in population biology (Princeton University Press).
25. West GB, Woodruff WH, Brown JH (2002) Allometric scaling of metabolic rate from molecules and mitochondria to cells and mammals. *Proc. Natl. Acad. Sci. USA* 99 Suppl 1:2473–2478.
26. Guckenheimer J, Holmes P (1983) *Nonlinear oscillations, dynamical systems, and bifurcations of vector fields* (Springer, New York).
27. Gross T, Feudel U (2004) Analytical search for bifurcation surfaces in parameter space. *Physica D* 195:292–302.
28. Hastings A (2001) Transient dynamics and persistence of ecological systems. *Ecol. Lett.* 4:215–220.
29. Neubert M, Caswell H (1997) Alternatives to resilience for measuring the responses of ecological systems to perturbations. *Ecology* 78:653–665.
30. Caswell H, Neubert MG (2005) Reactivity and transient dynamics of discrete-time ecological systems. *Journal of Difference Equations and Applications* 11:295–310.
31. Neubert M, Caswell H (2009) Detecting reactivity. *Ecology*.

**ACKNOWLEDGMENTS.** C.P.K was supported by the Omidyar Fellowship at the Santa Fe Institute

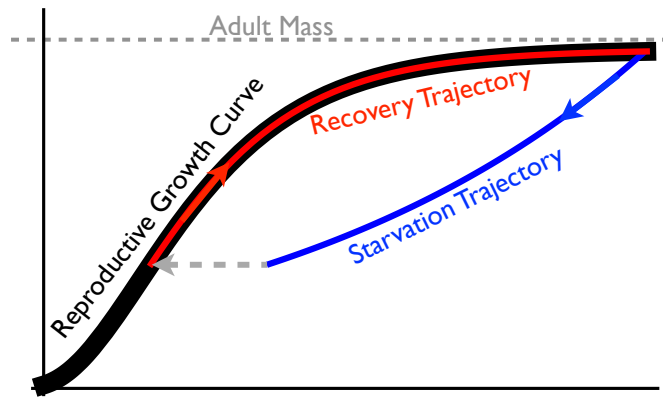


Fig. 1

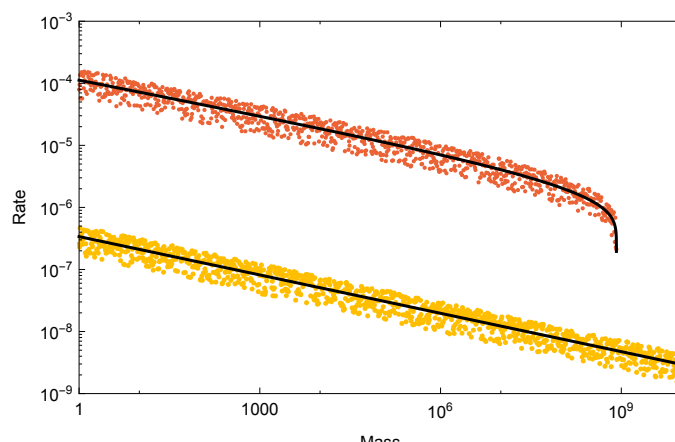


Fig. 2

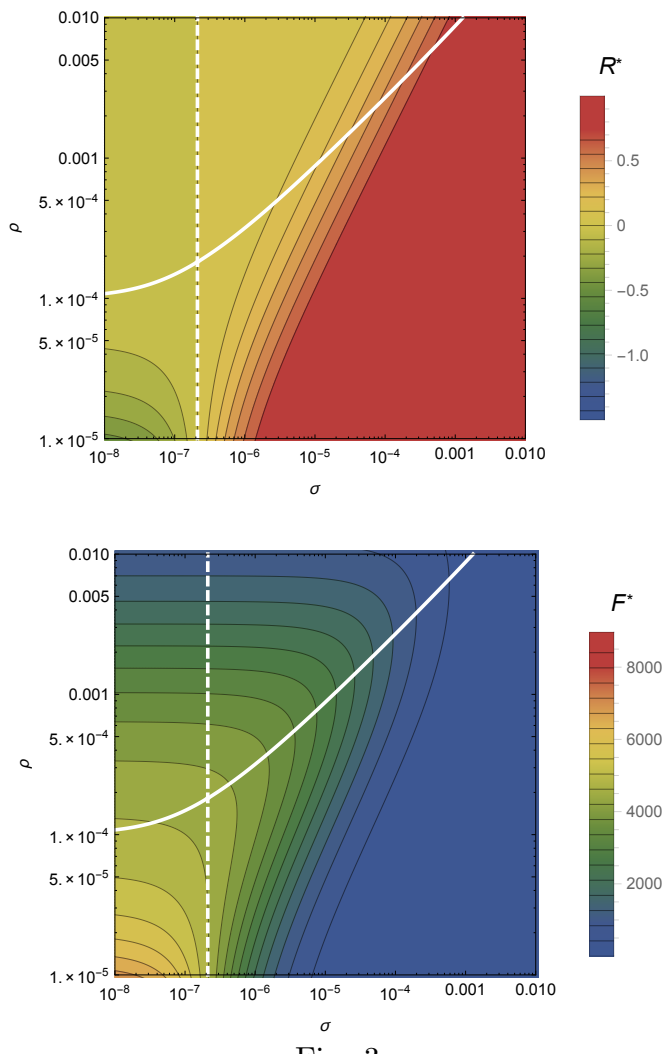


Fig. 3

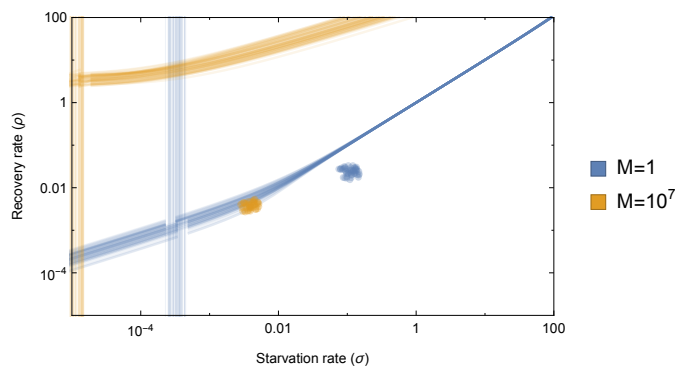


Fig. 4

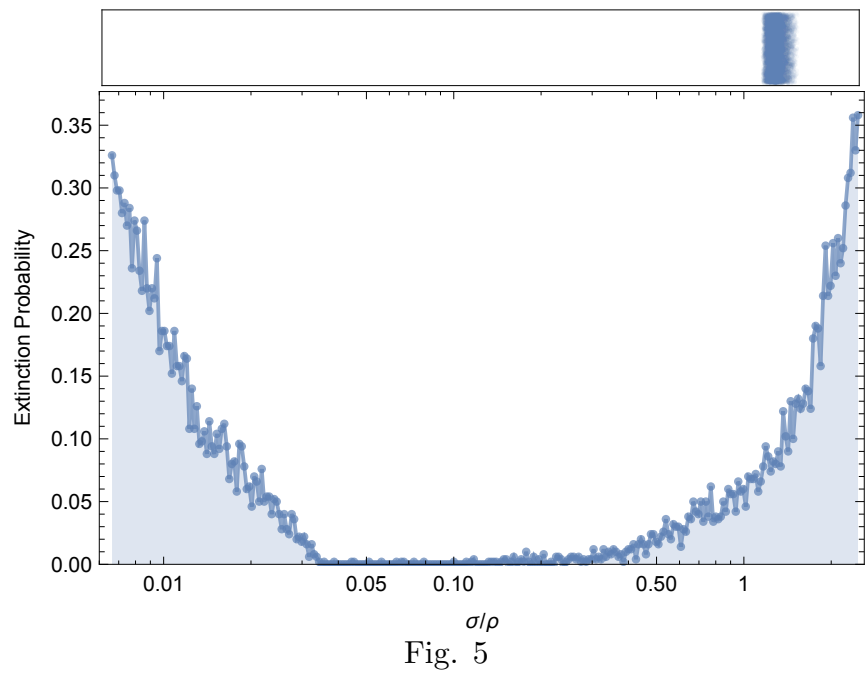


Fig. 5

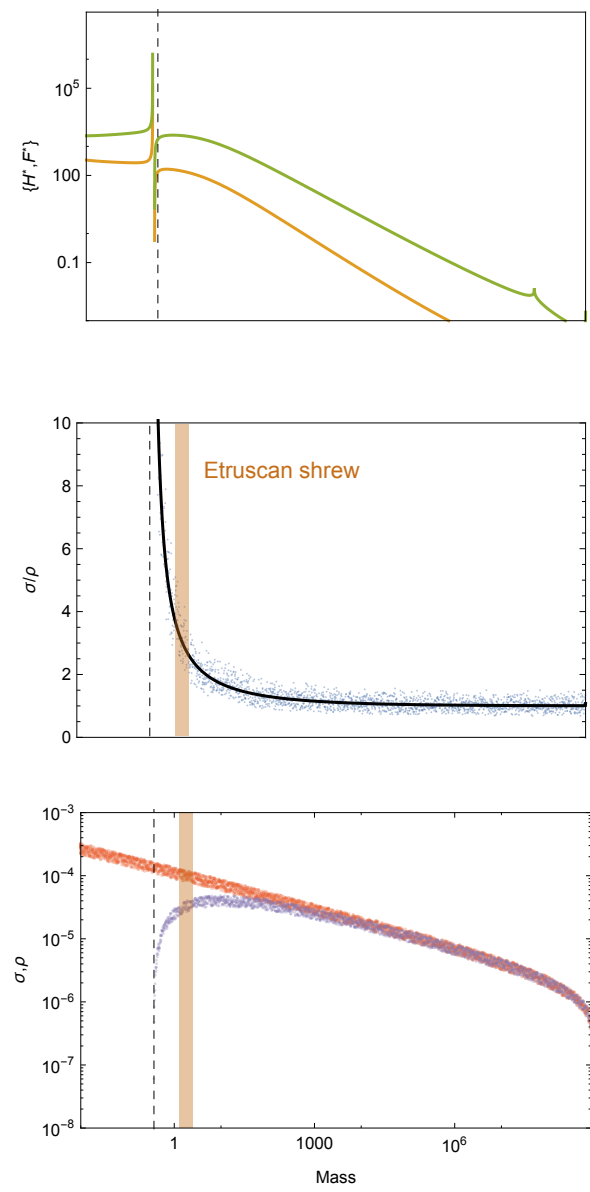


Fig. 6

Table 1: Parameter Values For Various Classes of Organisms

	Mammals	Unicellular karyotes	Eu- karyotes	Bacteria
$\eta$	3/4			1.70
$E_m$	10695 (J gram <sup>-1</sup> )			10695 (J gram <sup>-1</sup> )
$E'_m$	$\approx E_m$			$\approx E_m$
$B_0$	0.019 (W gram <sup>-<math>\alpha</math></sup> )			$1.96 \times 10^{17}$
$B_m$	0.025 (W gram <sup>-1</sup> )			0.025 (W gram <sup>-1</sup> )
$a$	$1.78 \times 10^{-6}$			$1.83 \times 10^{13}$
$b$	$2.29 \times 10^{-6}$			$2.29 \times 10^{-6}$
$\eta - 1$	-0.21			0.73
$\lambda_0$	$3.39 \times 10^{-7}$ (s <sup>-1</sup> gram <sup>1-<math>\eta</math></sup> )			56493
$\gamma$	1.19			0.68
$f_0$	0.02			$1.30 \times 10^{-5}$
$\zeta$	1.01			
$mm_0$	0.32			